**Proceedings of the ASME 2014 Dynamic Systems and Control Conference**
**DSCC2014**
**October 22-24, 2014, San Antonio, TX, USA**

**DSCC2014-6232**

# OPTIMAL UAV SENSOR MANAGEMENT AND PATH PLANNING FOR TRACKING MULTIPLE MOBILE TARGETS

**Negar Farmani*, Liang Sun, Daniel Pack**
Department of Electrical and Computer Engineering
The University of Texas at San Antonio
San Antonio, Texas 78249
Email: fkv344@my.utsa.edu, (liang.sun,daniel.pack) @utsa.edu

## ABSTRACT

In this paper, we present an optimal sensor manager and a path planner for an Unmanned Aerial Vehicle (UAV) to geo-localize multiple mobile ground targets. A gimbaled camera with a limited field of view (FOV) and a limited range is used to capture targets, whose states are estimated using a set of Extended Kalman Filters (EKFs). The sensor management is performed using a dynamic weighted graph and a Model Predictive Control (MPC) technique, determining the optimal gimbal pose that minimizes the overall uncertainty of target states. A UAV path planner that maximizes a novel cost function is employed to support the sensor management. Simulation results show the effectiveness of the proposed sensor manager and the path planner.

## INTRODUCTION

The ever increasing commercial and military applications of UAVs have been receiving considerable attention by a number of academic communities in recent years, especially due to UAVs' potential ability to reliably operate autonomously. Suitable UAV applications are surveillance, ocean exploration, search and rescue, and natural disaster assessment, just to name a few. A smart path planning is one of the most critical capabilities for UAVs to achieve any of these tasks. This capability becomes highlighted in tasks such as search and rescue when the emphasis is on early detection of targets. In the scenario where a UAV tracks multiple mobile ground targets, limitations on sensor coverage make tracking and path planning more challenging.

Significant advances have been reported to address the problem of tracking multiple mobile targets with a limited number of sensors. Sharma and Pack [1] presented a cooperative sensor resource management method to geo-localize multiple mobile targets. Han and Desouza [2] developed a method for a UAV to geo-localize multiple targets using optic flow and a SIFT (Scale Invariant Feature Transformation) based algorithm. Siam et al. [3] presented a method to detect and track multiple moving targets. They used a density-based spatial clustering algorithm to detect targets and Kalman Filters to estimate target state.

For the path planning task, efforts to plan the UAV paths in order to minimize the overall traveled distance have been reported [4], [5]. For target search, the objective of maximizing the probability of detecting targets is typically used [6], [7]. Sinha et al. [8] reported information optimization for a group of UAVs to track ground targets autonomously. Using the Fisher information, each UAV decides its path by maximizing a cost function based on its knowledge of neighboring UAVs' positions and targets. The results showed that the Root Mean Square Error (RMSE) of the position and velocity of targets decreased as the number of UAVs increased. Ruangwiset [9] proposed a method for a UAV to track a ground target by maintaining a constant horizontal distance between the target and the UAV. By considering a circle with its center as the target posi-

*Address all correspondence to this author.

tion and its radius as the desired relative distance, the UAV flew toward the circumference of the circle. Lin et al. [10] presented a method which uses an Unscented Kalman Filter to predict the target state and a Lyapunov vector field based algorithm for the UAV motion planning. Ragi and Chong [11] designed a path planning algorithm to guide UAVs for tracking multiple ground targets based on the theory of partially observable Markov decision processes (POMDPs). Yu et al. [12] presented a probabilistic path planning algorithm to track a moving target using a UAV in cooperation with an unmanned ground vehicle. The path planning algorithm was designed to maximize the sum of probability of detection over a finite look-ahead horizon. Baek et al. [13] optimized the path of a UAV to track a target moving slower than the minimum UAV speed. They used sequential decision processes and a grid-based Markov Decision Process (MDP) to find the optimal UAV trajectory while minimizing the location uncertainty of a mobile target.

This paper introduces a path planner of a UAV that optimizes the path of the UAV and minimizes the overall target position uncertainties. In particular, we consider a single UAV with a gimbaled camera tracking multiple mobile targets with aforementioned sensor limitations. The main contribution of this paper is the introduction of a sensor manager and a path planner for a single UAV tracking multiple targets. The sensor manager incorporates a novel technique which uses a Dynamic Weighted Graph (DWG) and Model Predictive Control (MPC) technique to determine the optimal gimbal configuration. The path planner uses a cost function that incorporates estimates of targets locations and the relative distances of the UAV from targets.

The rest of the paper is organized as follows. In the Background section, we give a brief description of coordinate frames, the camera image projection method and the geolocation technique used in the path planner and sensor manager. We describe the proposed UAV path planner and the sensor manager in the Control Design section. The Experimental Result section offers the analysis of simulation results for a single UAV tracking multiple targets, which is followed by some concluding remarks in the Conclusion section.

## BACKGROUND

In this section, we briefly describe the coordinate frames used to geo-localize ground targets based on work reported in [14]. The positions of the UAV and targets are represented in an inertial frame by $\mathbf{p}_u^i = [p_n^i, p_e^i, p_d^i]^T$ and $\mathbf{p}_k^i = [p_{kn}^i, p_{ke}^i, 0]^T$, respectively, where $n$ and $e$ represent the north and east directions, respectively, $k$ denotes the $k^{th}$ target and $i$ defines the inertial frame. The origins of the gimbal and the camera frames are assumed to be at the center of UAV mass. The body frame, $F_b \triangleq (i^b, j^b, k^b)$, the gimbal frame, $F_g \triangleq (i^g, j^g, k^g)$, and the camera frame, $F_c \triangleq (i^c, j^c, k^c)$, are three frames used to project

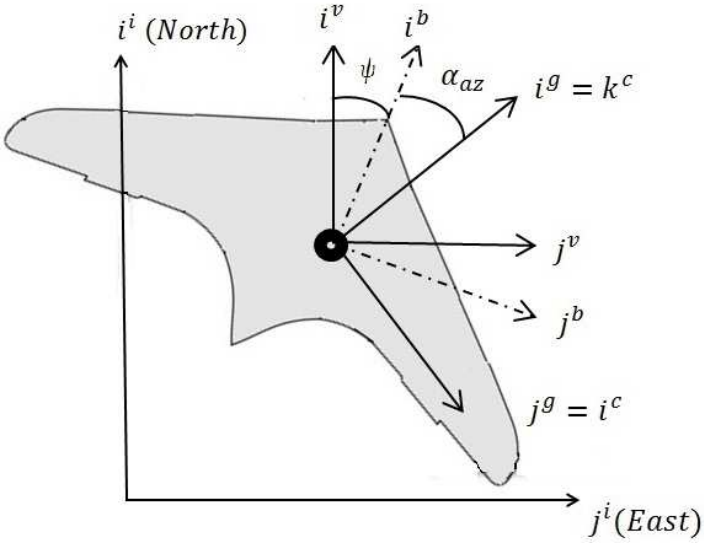


Figure 1. A top view depicting the relationships among the gimbal frame $(i^g, j^g, k^g)$, camera frame $(i^c, j^c, k^c)$ and vehicle body frame $(i^b, j^b, k^b)$.

captured targets in a 3D space onto the image plane. As shown in Fig. 1 and Fig. 2, the rotation matrix $R_b^g$ that relates the body frame to the gimbal frame is given by

$$R_b^g \triangleq \begin{pmatrix} \cos\alpha_{el}\cos\alpha_{az} & \cos\alpha_{el}\sin\alpha_{az} & -\sin\alpha_{el} \\ -\sin\alpha_{az} & \cos\alpha_{az} & 0 \\ \sin\alpha_{el}\cos\alpha_{az} & \sin\alpha_{el}\sin\alpha_{az} & \cos\alpha_{el} \end{pmatrix}, \quad (1)$$

where $\alpha_{az}$ and $\alpha_{el}$ are the azimuth and elevation angles of the gimbal with respect to the UAV body frame. The $R_g^c$ which relates the gimbal frame to the camera frame is represented by

$$R_g^c \triangleq \begin{pmatrix} 0 & 1 & 0 \\ 0 & 0 & 1 \\ 1 & 0 & 0 \end{pmatrix}. \quad (2)$$

The target location is described in the camera frame and projected into pixels ( $\varepsilon_x$ , $\varepsilon_y$) on the image plane. The desired direction of the optical axis to point to target $k$ in the camera frame which determines the gimbaled camera pointing direction, $\check{l}_d^c$, is given by

$$\check{l}_d^c = \frac{\mathbf{l}}{L} = \frac{1}{F}\begin{pmatrix} \varepsilon_x \\ \varepsilon_y \\ f \end{pmatrix}, \quad (3)$$

where $f$ is the focal length of the camera, $L = ||\mathbf{p}_k - \mathbf{p}_u||$, and

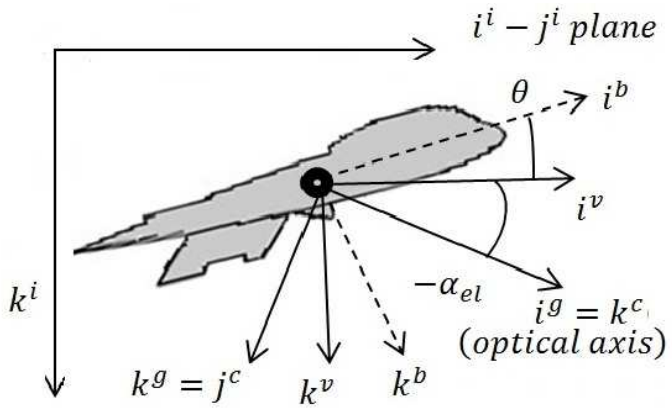


Figure 2. A side view depicting the relationships among the gimbal frame $(i^g, j^g, k^g)$, camera frame $(i^c, j^c, k^c)$ and vehicle body frame $(i^b, j^b, k^b)$.

$F$ is defined as

$$F \triangleq \sqrt{{\varepsilon_x}^2 + {\varepsilon_y}^2 + f^2}. \tag{4}$$

The desired direction of the optical axis in the body frame can be calculated by

$$\check{l}_d^b = \begin{pmatrix} \check{l}_{xd}^b \\ \check{l}_{yd}^b \\ \check{l}_{zd}^b \end{pmatrix} = R_g^b R_c^g \check{l}_d^c. \tag{5}$$

The control inputs for the gimbal's azimuth angle, $u_{az}$, and the gimbal's elevation angle, $u_{el}$, are given by

$$\begin{aligned} u_{az} &= k_{az}(\alpha_{az}^c - \alpha_{az}) \\ u_{el} &= k_{el}(\alpha_{el}^c - \alpha_{el}), \end{aligned} \tag{6}$$

where $k_{az}$ and $k_{el}$ are control gains and $\alpha_{az}^c$ and $\alpha_{el}^c$ are desired command angles which can be calculated by

$$\begin{aligned} \alpha_{az}^c &= \tan^{-1}\left(\frac{\check{l}_{yd}^b}{\check{l}_{xd}^b}\right) \\ \alpha_{el}^c &= \sin^{-1}(\check{l}_{zd}^b). \end{aligned} \tag{7}$$

## Geo-localization

In this section, we describe the process used to estimate positions and velocities of mobile targets. We assume that the UAV is equipped with a noisy Global Positioning System (GPS) sensor and an Inertial Measurement Unit (IMU) sensor. Target positions in the inertial coordinate can be calculated by applying the following image projection transformation

$$\mathbf{p}_k^i = \mathbf{p}_u^i + L\left(R_b^i R_g^b R_c^g \check{l}_k^c\right), \tag{8}$$

where $\check{l}_k^c$ is the normal vector of target $k$ with respect to the camera frame and

$$R_b^i \triangleq \begin{pmatrix} c_\theta c_\psi & c_\theta s_\psi & -s_\theta \\ s_\phi s_\theta c_\psi - c_\phi s_\psi & s_\phi s_\theta s_\psi + c_\phi c_\psi & s_\phi c_\theta \\ c_\phi s_\theta c_\psi + s_\phi s_\psi & c_\phi s_\theta s_\psi - s_\phi c_\psi & c_\phi c_\theta \end{pmatrix} \tag{9}$$

with $c_\theta \triangleq \cos(\theta)$ and $s_\theta \triangleq \sin(\theta)$. The angels $\phi, \theta, \psi$ are roll, pitch and yaw angles of the UAV, respectively.

To estimate the positions and velocities of targets, the motion model for the $i^{th}$ target is defined as

$$\dot{x_i} = y_i(x_i, u) + q(t). \tag{10}$$

$x_i = [x_{ni}, x_{ei}, v_{ni}, v_{ei}, L_i]^T$ is the state of target $i$, where $x_{ni}$, $x_{ei}$, $v_{ni}$ and $v_{ei}$ are the $i^{th}$ target's position and velocity in the north and east directions, respectively. $L_i$ is the range between the $i^{th}$ target and the UAV and $y_i = \left(v_{ni}, v_{ei}, 0, 0, \dot{L}_i\right)^T$ and $q(t)$ is the motion model Gaussian noise.

For each target $x_i$, the prediction step of the estimation used by the Extended Kalman Filter (EKF) at time step $k$ is given by

$$\begin{aligned} \widehat{x}_k &= \widehat{x}_{k-1} + T_s y_i(\widehat{x}_{k-1}, u_k) \\ P_k^- &= P_{k-1}^+ + T_s(A_{k-1}P_{k-1}^+ + P_{k-1}^+ A_{k-1}^T + Q) \end{aligned} \tag{11}$$

where $\widehat{x}$ is the estimated state, $A = \frac{\partial y}{\partial x}(\widehat{x}, u)$ is the system Jacobian matrix, $P_k$ is the state covariance matrix, $T_s$ is the sampling period and $+/-$ superscripts represent after and before measurement updates. $Q$ is the covariance matrix of $q(t)$. The measurement model is given by $h(x) = p_k - LR_b^i R_g^b R_c^g \check{l}_d^c$. The measurement update of EKF is governed by

$$\begin{aligned} C_k &= P_k^- H_k^T (R + H_k P_k^- H_k^T)^{-1} \\ P_k^+ &= (I - C_k H_k) P_k^- \\ \widehat{x}_k &= \widehat{x}_k + C_k(z_k - h(\widehat{x}_k, u_k)), \end{aligned} \tag{12}$$

where $H = \frac{\partial h}{\partial x} = [I\ R_b^i R_g^b R_c^g \check{l}^c]$ is the measurement Jacobian matrix, $C$ is the Kalman gain, $R$ is the sensor covariance, ans $z$ is the actual measurement.

We assume the following dynamics for the UAV. With a constant airspeed, $V_a$, and zero wind speed, the equations of the UAV motion are calculated by

$$\begin{pmatrix} \dot{p_n} \\ \dot{p_e} \\ \dot{h} \end{pmatrix} = V_a \begin{pmatrix} \cos\psi \\ \sin\psi \\ 0 \end{pmatrix}. \tag{13}$$

The coordinated turn condition in terms of the heading angle ($\psi$) and constant airspeed is given by

$$\dot{\psi} = \frac{g\tan\phi}{V_a}, \tag{14}$$

where

$$\dot{\phi} = k_\phi(\phi^c - \phi_i), \tag{15}$$

$g$ is the gravitational acceleration, $k_\phi$ is a positive constant and

$$\phi^c = \tan^{-1}\left(\frac{p_{ke} - p_e}{p_{kn} - p_n}\right). \tag{16}$$

## OPTIMAL SENSOR MANAGER AND PATH PLANNER

In this section we describe the optimal sensor manager and the path planner for tracking multiple mobile ground targets. The target movements are assumed to be random with constant velocities. The UAV also flies with a constant velocity greater than the target's. We assume that the UAV is equipped with a gimbaled camera that has a limited field of view and a limited sensing range. The images collected from the camera are used to estimate positions and velocities of targets.

### Gimbal Control

The optimization criteria for the camera sensor manager is the overall target location uncertainties. In order to minimize the overall uncertainty, we use a Dynamic Weighted Graph (DWG) along with an optimization function to determine the pointing direction of the gimbal frame. In this method, we first define a graph $G \triangleq [g_{ij}] \in \Re^{n\times n}$, representing the distance relations among targets. Each element of matrix $G$ is given by

$$g_{ij} = \begin{cases} 0 & \text{if } i = j \\ \frac{e^{-|d_{ij}|}}{\sqrt{(\delta_{x_i}+\delta_{x_j})^2+(\delta_{y_i}+\delta_{y_j})^2}}, & \text{if } i \neq j \end{cases} \tag{17}$$

where $d_{ij}$ represents the estimated distance between targets $i$ and $j$, $\delta_{x_i}$, $\delta_{x_j}$, $\delta_{y_i}$ and $\delta_{y_j}$ are estimated position variances of targets $i$ and $j$ in the north and east directions, respectively.

For each pair of targets, the numerator of Eqn. (17) awards targets that are close to each other. It describes the exponentially decaying relationship between the $i^{th}$ and $j^{th}$ as the distance between them increases. The denominator incorporates the uncertainties of position estimations of both the $i^{th}$ and $j^{th}$ targets. The resulting graph is a weighted symmetric matrix with estimated distance among targets. To find the optimal pointing direction for the gimbal, we first sum each column (or row) of $G$. The $i^{th}$ column sum represents the density of targets near target $i$. A large summation implies more targets are in proximity of target $i$. Comparing the summation of each column of $G$, we select the $n$ largest column sums as camera gimbal pose candidates.

After the candidates are generated, we apply the sensor constraint to determine whether or not the camera can capture the desired number of targets within its FOV. Solving the question, however, depends on a pre-determined camera pose. We use the mean between the $i^{th}$ target and its closest neighbor as the camera gimbal pointing direction, and using the camera FOV constraint, determine the number of targets that can be captured. The targets captured in the current FOV are evaluated later using a Model Predictive Control (MPC) based optimization technique before a final gimbal pointing direction is found. The MPC function which is designed to minimize the overall uncertainty of targets is given by

$$\text{minimize} \prod_{i=1}^{n} tr(P_i^{-1} + a_i H^T R^{-1} H)^{-1} \tag{18}$$

$$\textstyle\sum_{i=1}^{n_{FOV}} a_i = \text{number of targets in FOV},$$

where $a_i \in \{0,1\}$ and $n_{FOV}$ is the number of targets within the FOV. The function shown in Eqn. (18) is designed to minimize the target uncertainties and the uncertainty generated by the onboard sensor. The inverse of covariance matrix $P_i$, known as the information matrix, shows the amount of information we have on target $i$ and $H^T R^{-1} H$ describes the information 'gains' that the UAV will have if it chooses to capture target $i$ using the onboard sensor with its sensor noise characteristic. By taking the inverse of the arguments in Eqn. (18), we obtain the combined covariance. The trace of the resulting matrix again captures overall covariance of all targets. The multiplication operator is used to amplify the difference between gimbal pose candidates. Finding the minimum of the overall expression leads to an optimal gimbal pose.

### Path Planner

The real-time path planner uses the cost function described in Eqn. (19), which incorporates the uncertainty of state estimations and distances of the UAV from targets, to determine a path

toward a target.

$$\text{maximize} \sum_{i=0}^{n_t} f\left(P_i, d_{i,i+1}, \frac{dP_i}{dt}\right). \tag{19}$$

In Eqn. (19), $n_t$ defines the estimated number of targets, the $0^{th}$ target denotes the UAV, $P_i$ is the covariance matrix of target $i$, $d_{i,i+1}$ is the distance between target $i$ and target $i+1$ . The time derivative of covariance matrix for target $i$ is represented by $\frac{dP_i}{dt}$, where $P_0 = \frac{dP_0}{dt} = 0$.

It is noted that as $n_t$ increases, the computational complexity will also increase. We used two time horizon steps of the UAV path. The cost function in Eqn. (19), then, is the sum of two parts with the first part given in Eqn. (20). First part of cost function consists of the uncertainty of target $i$, the distance between target $i$ and the UAV, and the cumulation of the time derivative of the covariance matrix of target $i$ over the estimated time for the UAV to reach target $i$, in the north and east directions, respectively.

$$f_1(P_i, d_{ui}, \frac{dP_i}{dt}) = w_1|P_i| + w_2\frac{1}{d_{ui}} + w_3(\int_0^{t_{ui}} \dot{P}_{ix}(t)\dot{P}_{iy}(t)dt). \tag{20}$$

In Eqn. (20), $|P_i|$ is the determinant of the covariance matrix of target $i$. This term reflects the idea that a target with a larger uncertainty will contribute more information if it is observed. The second term, $\frac{1}{d_{ui}}$, the inverse of distance between the UAV and the $i^{th}$ target, awards a target that is closer to the UAV and the last term in Eqn. (20) incorporates the target $i$'s cumulative position uncertainty variation in the north and east directions, respectively. The target with a large rate of change of covariance contributes more to the cost function. The multiplication inside the integral combines both the north and east direction variances. $t_{ui}$ is the traveled time for UAV to reach target $i$ which is given by

$$t_{ui} = \frac{d_{ui}}{V_a}. \tag{21}$$

Finally, $w_1, w_2$ and $w_3$ are chosen based on the importance of each term. In our implementation, we normalize each term in Eqn. (20) to find the weights.

The second part of the cost function considers the cost of a path after the UAV has reached the first target $i$.

$$f_2\left(P_j, d_{ij}, \frac{dP_j}{dt}\right) = e^{-\beta t_{uj}}\left(w_1|P_j| + w_2\frac{1}{d_{ij}} + w_3\int_0^{t_{uj}} \dot{P}_{jx}(t)\dot{P}_{jy}(t)dt\right). \tag{22}$$

Similar to Eqn. (20), in Eqn. (22), $|P_j|$ is the determinant of the covariance matrix of target $j$, term $\frac{1}{d_{ij}}$ is the inverse of the distance between targets $i$ and $j$ which shows the cost involved for the UAV to capture target $j$ after reaching target $i$, and the last term contains the change of covariance in the north and east directions of target $j$, respectively. As it takes time for UAV to reach target $i$ and then fly toward target $j$, we take the integral of position covariance of target $j$ over time, $t_{uj}$, that the UAV spend to travel to target $j$. $t_{uj}$ can be calculated as

$$t_{uj} = \frac{d_{ui} + d_{ij}}{V_a}. \tag{23}$$

Weights $w_1, w_2$ and $w_3$ have the same meanings as in Eqn. (20). We apply the exponential function in Eqn. (22) to reflect the decreasing value of the cost based on the expected time delay for the UAV to reach target $j$ via target $i$.

Using the cost function combining Eqn. (20) and Eqn. (22), the UAV finds a path with the maximum cost. The process is repeated in each iteration as the covariance matrix and target positions are updated.

## EXPERIMENTAL RESULTS

In this section, we present the MATLAB simulation results to show the effectiveness of the proposed sensor manager and the path planner by comparing its performance with the ones using only the sensor manager and the rudimentary path planner. We first show the result when the UAV only used the sensor manager with a crude path planner that directs the UAV to the location pointed by the gimbal without any optimization employed. We call this approach as"Method 1" in the rest of the paper. In what we call the "Method 2", both sensor manager and the path planner are implemented. The destination for the UAV is a target which is determined by the cost function defined in Eqn. (19). Both methods have the same UAV and sensor constraints. We assume a single UAV equipped with a gimbaled camera with a limited FOV and a limited sensing range tracking five mobile ground targets in an urban environment. The experiment was performed 100 times, each run lasting for 100 seconds. The initial target and the UAV positions in each run were assigned randomly but then locations

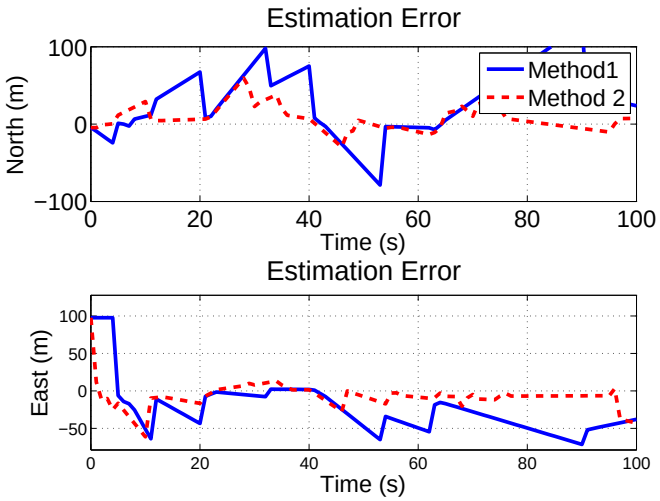


Figure 3. A SAMPLE EXPERIMENTAL RUN: TARGET 1 GEO-LOCATION ERRORS RESULTED FROM RUNNING METHOD 1 AND METHOD 2.

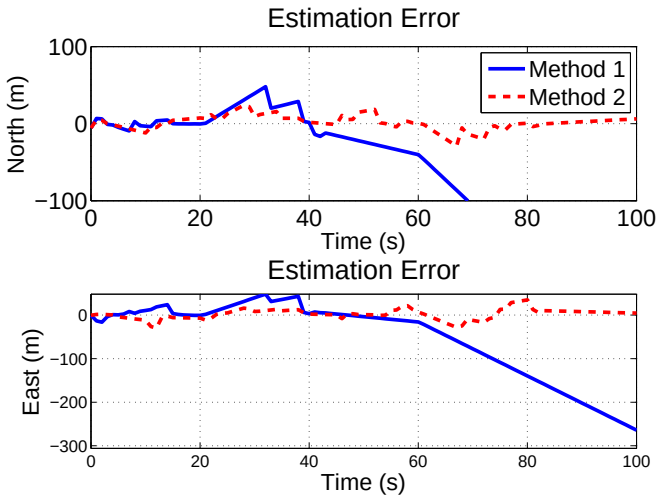


Figure 4. A SAMPLE EXPERIMENTAL RUN: TARGET 2 GEO-LOCATION ERRORS RESULTED FROM RUNNING METHOD 1 AND METHOD 2.

and the target motion were identical for both methods. Targets moved in a piece-wise linear fashion with a constant speed (5m/s). The UAV flew at an altitude of 100 (m) with a constant speed (13m/s). We selected the camera range of 250 (m) and assumed that two seconds are needed for the gimbal to move the mechanical parts to change its pose.

Figures 3 - 7 present the results of geo-location errors from running both methods. The figures show the geo-localization errors of five targets in the north and east directions, respectively. Results of Method 2 (dashed line) and Method 1 (solid line) are shown in each figure. It is clear from the figures that the error variations resulted from Method 2 are smaller and smoother than the ones from Method 1. This improvement is due to the use of the optimal path planner.

Table. 1 shows the average errors of each target position estimation in the north and east directions, respectively, for 100 experiments using both methods. Table. 2 shows the overall position estimation errors of five targets in the north and east directions, respectively. The numerical results and the percentage difference between two methods confirm the improvements of Method 2.

Finally, Fig. 8 shows the target movements and the UAV trajectory for a sample experimental run. The UAV path using Method 1 stayed in a circular path but the path of the UAV using Method 2 was regulated according to the optimal solution of Eqn. (19).

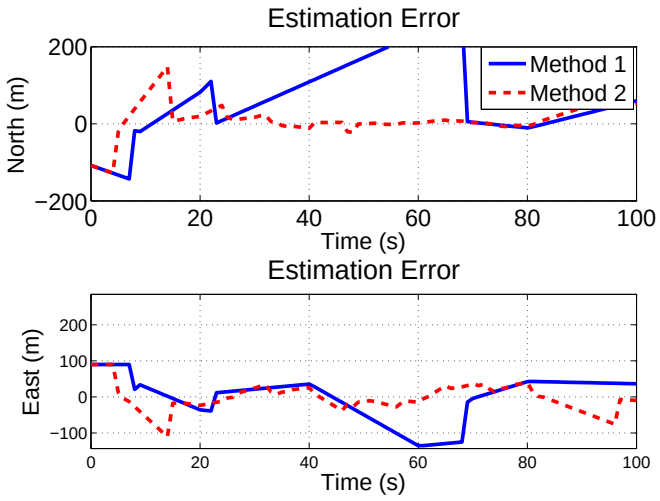


Figure 5. A SAMPLE EXPERIMENTAL RUN: TARGET 3 GEO-LOCATION ERRORS RESULTED FROM RUNNING METHOD 1 AND METHOD 2.

## CONCLUSION

In this paper we proposed and demonstrated a new sensor manager and a path planner for a single UAV to track multiple mobile ground targets. We used a Dynamic Weighted Graph to represent the target position distribution and a Model Predictive Control technique to optimize the gimbaled camera pose. A novel cost function which incorporates the uncertainty of targets and the relative distance of UAV from targets is used to find an optimal path for the UAV. The numerical results obtained

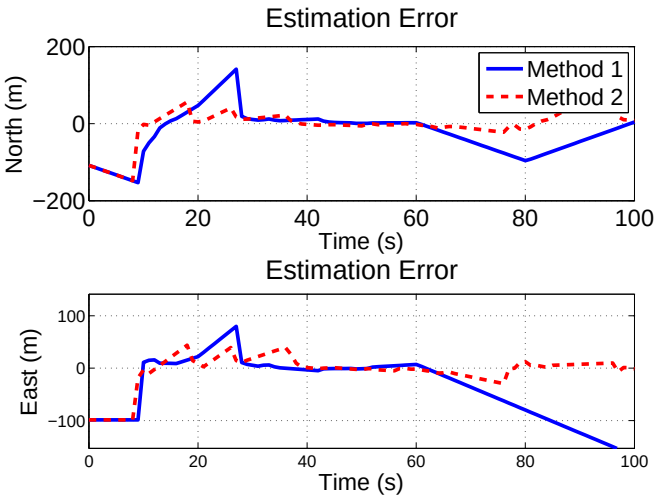


Figure 6. A SAMPLE EXPERIMENTAL RUN: TARGET 4 GEO-LOCATION ERRORS RESULTED FROM RUNNING METHOD 1 AND METHOD 2.

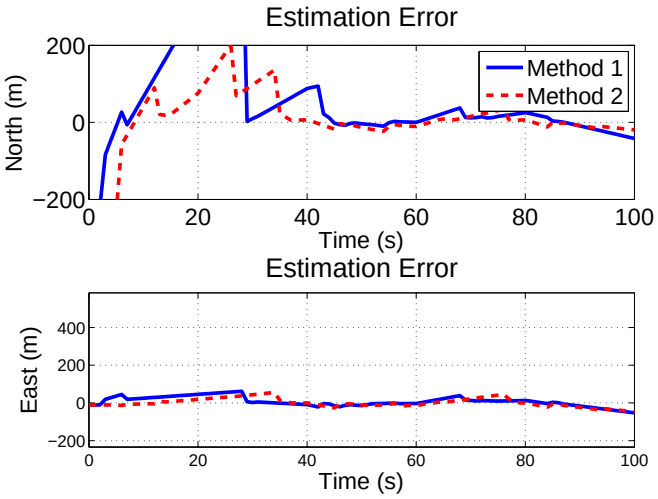


Figure 7. A SAMPLE EXPERIMENTAL RUN: TARGET 5 GEO-LOCATION ERRORS RESULTED FROM RUNNING METHOD 1 AND METHOD 2.

from the overall system with both the sensor manager and the path planner show the improvements over the ones using only the optimal sensor manager. We plan to extend the sensor manager and the path planner to a team of UAVs tracking multiple targets cooperatively.

Table 1. AVARAGE TARGET GEO-LOCATION ERRORS(FIVE TARGETS) IN THE NORTH AND EAST DIRECTIONS BASED ON 100 EXPERIMENTS USING THE METHOD 1 AND METHOD 2.

| Target No. | 1 | 2 | 3 | 4 | 5 |
|---|---|---|---|---|---|
| Position North Error (m) (Method 2) | 22.4 | 21.1 | 37.7 | 65.9 | 190 |
| Position North Error (m) (Method 1) | 37.4 | 24.6 | 130.3 | 91.3 | 925.7 |
| Position East Error(m) (Method 2) | 25.2 | 17 | 33.2 | 47.8 | 42.5 |
| Position East Error (m) (Method 1) | 37.4 | 23 | 103 | 66.1 | 90.2 |

Table 2. OVERALL AVERAGE TARGET GEO-LOCATION ERRORS IN THE NORTH AND EAST DIRECTIONS.

| Overall Error | Error | Difference (%) |
|---|---|---|
| Overall Position North Error (m) (Method 2) | 67.4 | 72 |
| Overall Position North Error (m) (Method 1) | 241.86 | |
| Overall Position East Error (m) (Method 2) | 33.14 | 51 |
| Overall Position East Error (m) (Method 1) | 63.94 | |

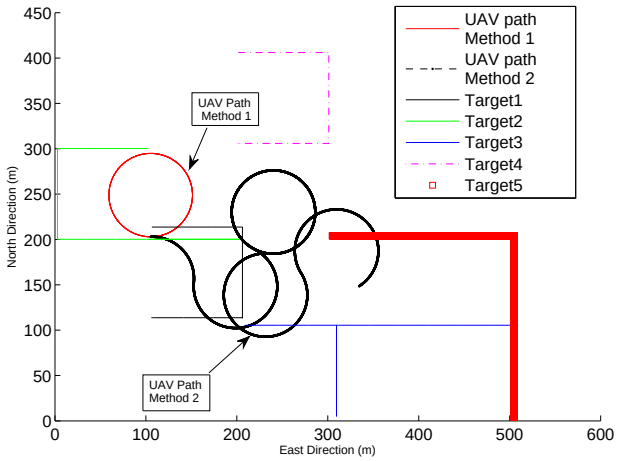


Figure 8. TRAJECTORIES TARGETS AND UAV.

## REFERENCES

[1] Sharma, R., and Pack, D., 2013. "Cooperative sensor resource management to aid multi target geolocalization using a team of small fixed-wing unmanned aerial vehicles". In AIAA Guidance, Navigation, and Control (GNC) Conference.

[2] Han, K., and DeSouza, G., 2009. "Multiple targets geolocation using sift and stereo vision on airborne video sequences". In Intelligent Robots and Systems, 2009. IROS 2009. IEEE/RSJ International Conference on, pp. 5327–5332.

[3] Siam, M., ElSayed, R., and ElHelw, M., 2012. "On-

board multiple target detection and tracking on camera-equipped aerial vehicles". In Robotics and Biomimetics (ROBIO), 2012 IEEE International Conference on, pp. 2399–2405.

[4] Sujit, P. B., and Beard, R., 2009. "Multiple UAV path planning using anytime algorithms". In Proceedings of the 2009 Conference on American Control Conference, ACC'09, IEEE Press, pp. 2978–2983.

[5] Rathinam, S., and Sengupta, R., 2006. "Lower and upper bounds for a multiple depot UAV routing problem". In Decision and Control, 2006 45th IEEE Conference on, pp. 5287–5292.

[6] Martin, S., and Newman, A., 2008. "The application of particle swarm optimization and maneuver automatons during non-Markovian motion planning for air vehicles performing ground target search". In Intelligent Robots and Systems, 2008. IROS 2008. IEEE/RSJ International Conference on, pp. 2605–2610.

[7] Roy, N., and Earnest, C., 2006. "Dynamic action spaces for information gain maximization in search and exploration". In American Control Conference, pp. 1631–1636.

[8] Sinha, A., Kirubarajan, T., and Bar-Shalom, Y., 2005. "Autonomous ground target tracking by multiple cooperative UAVs". In Aerospace Conference, 2005 IEEE, pp. 1–9.

[9] Ruangwiset, A., 2009. "Path generation for ground target tracking of airplane-typed UAV". In Robotics and Biomimetics, 2008. ROBIO 2008. IEEE International Conference on, pp. 1354–1358.

[10] Wang, L., Li, Y., Zhu, H., and Shen, L., 2010. "Target state estimation and prediction based standoff tracking of ground moving target using a fixed-wing UAV". In Control and Automation (ICCA), 2010 8th IEEE International Conference on, pp. 273–278.

[11] Ragi, S., and Chong, E. K. P., 2012. "Dynamic UAV path planning for multitarget tracking". In American Control Conference (ACC), 2012, pp. 3845–3850.

[12] Yu, H., Beard, R., Argyle, M., and Chamberlain, C., 2011. "Probabilistic path planning for cooperative target tracking using aerial and ground vehicles". In American Control Conference (ACC), 2011, pp. 4673–4678.

[13] Baek, S., Kwon, H., Yoder, J., and Pack, D., 2013. "Optimal path planning of a target-following fixed-wing UAV using sequential decision processes". In Intelligent Robots and Systems (IROS), 2013 IEEE/RSJ International Conference on, pp. 2955–2962.

[14] Beard, R., and McLainTimothy, W., 2012. *Small Unmanned Aircraft: Theory and Practice*. Princeton University Press.